Minimally Invasive Approach for Diagnosing TMJ Osteoarthritis

B. Shoukri, J.C. Prieto, A. Ruellas, M. Yatabe, J. Sugai, M. Styner, H. Zhu, C. Huang, B. Paniagua, S. Aronovich, L. Ashman, E. Benavides, P. de Dumast, N.T. Ribera, C. Mirabel, L. Michoud, Z. Allohaibi, M. Ioshida, L. Bittencourt, L. Fattori, L.R. Gomes, and L. Cevidanes

Appendix

Materials and Methods:

Inclusion and Exclusion Criteria:

The inclusion criteria were subjects over the age of 21 and have a diagnosis (within 10 years) of TMJOA. The exclusion criteria were: growing subjects; presence of a congenital syndrome affecting the maxillofacial complex; history of facial trauma or surgery; systemic medical condition involving the immune system; degenerative musculoskeletal disease; and women of child-bearing age that are pregnant. Subjects were not excluded on the basis of gender, race, or ethnicity.

Serum and Salivary Collection:

Saliva and blood samples were obtained at the same appointment that the hr-CBCT scans were taken. 5ml of venous blood was collected in an ethylenediaminetetraacetic acid (EDTA) tube. Whole blood was centrifuged for 20 minutes at 1000 revolutions per minute (RPM) to extract serum and then aliquoted for future analysis of biological markers expression. Subjects were given a 14ml sterile test tube with a funnel inserted; they were instructed to tilt their head forward allowing the unstimulated saliva to drip off their lower lip and into the funnel/test tube until 2ml was collected. Protease inhibitors were added to the sample; 20µl aprotinin and 10µl phenylmethylsulfonyl fluoride (PMSF). The vials were vortexed for at least 5-10 seconds and then placed in matrix racks/white freezer boxes, and immediately stored at -80°C. The collection of unstimulated saliva and the inclusion of a protease inhibitor cocktail was similar as done in Kaczor-Urbanowicz et al. 2018 (Kaczor-Urbanowicz et al. 2018).

Serum and Salivary Measurements:

The levels of protein markers of nociception, inflammation, angiogenesis and bone resorption, as shown in Appendix Table 1 were quantified. The Custom human Quantibody® protein microarrays are an array-based multiplex sandwich Enzyme-Linked Immunosorbent Assay (ELISA) system for simultaneous quantitative measurement of the concentration of multiple proteins. Like a traditional ELISA, it uses a pair of antigen-specific antibodies to capture the protein of interest. The RayBiotech Quantibody® system was chosen to carry out the protein assays because it combines the high sensitivity and specificity of ELISA and the high throughput of arrays (RayBiotech 2018). Glass slides were used that had 16 wells each with identical cytokine antibody arrays. The use of biotinylated antibodies helps recognize a different epitope of the target cytokine; and a streptavidin-conjugated equivalent dye allows for detection levels for the specific proteins to be visualized using a fluorescence laser scanner (RayBiotech 2018).

hr-CBCT Imaging Details:

The CBCT imaging acquisition protocol consisted of: a field of view of 40mm x 40mm, high resolution scanning mode, 90 kV, 87.5 mAs, 30.8s, 80µm voxel size, and an effective dose of 43µSv (Ludlow et al. 2014).

Shape Variation Analyzer in Slicer Software:

The ShapeVariationAnalyzer's (SVA) (de Dumast et al. 2018) module of the Slicer software, a freely accessible source code found on GitHub (de Dumast 2017), was used for automatic classification of morphological variation in TMJOA based on the NN.

Statistical Analysis:

Descriptive statistics were used to calculate the means, standard deviations, and p-values between the two groups for each biomarker (Appendix Table 3). Independent Student's t-tests compared the mean levels of protein expression in the TMJOA and control groups. Statistical significance was pre-set at $\alpha = 0.05$. The accuracy of the NN classification of condylar morphological variability and the repeated clinicians' consensus were assessed using confusion matrices, also known as error or contingency matrices (Stehman 1997). We used Principal Component Analysis (PCA) to select the variables highly correlated with the first principal components in each group (Appendix Table 2). Bonferroni correction or the false discovery rate (FDR) method (Benjamini 2010) was implemented to correct for multiple comparisons. A FDR of 0.2 was applied.

Appendix Table 1: Biomarkers that have been associated with 3D surface morphology changes of the mandibular condyle in TMJOA subjects. 3D, three-dimensional; TMJOA, temporomandibular joint osteoarthritis.

Biomarker	Description
6Ckine	Has been shown to be produced by vascular endothelium (Gunn et al. 1998). 6Ckine has angiostatic properties (Soto et al. 1998). It can trigger rapid integrin-dependent arrest of lymphocytes rolling under physiological shear and is highly expressed by high endothelial venules (Campbell et al. 1998).
ANG	Induces angiogenesis by activating vessel endothelial and smooth muscle cells; and triggers a number of biological processes, including cell migration, invasion, proliferation, and formation of tubular structures (Gao and Xu 2008). A potential role for angiogenin (ANG) in inflammatory conditions is supported by its angiogenic activity and acts as a regulatory cytokine (Liote et al. 2003).
BDNF	Reported to be involved in the joint inflammatory process and its production is increased in response to pro-inflammatory cytokines (Grimsholm et al. 2008). Animal models have shown joint inflammation and arthritis demonstrate increased BDNF expression in the synovial tissue of those joints and their associated dorsal root ganglions (Kras et al. 2013).
CXCL16	A transmembrane adhesion molecule on the surface of antigen presenting cells and a soluble chemoattractant for activated T cells (Abel et al. 2004).
ENA-78	A potent chemoattractant and activator of neutrophils (Keelan et al. 2004). It is produced following stimulation of cells with the inflammatory cytokines IL-1 or tumor necrosis factor-alpha. ENA-78 stimulates the chemotaxis of neutrophils possesses angiogenic properties and has been implicated in connective tissue remodeling (Chang et al. 1994).
GM-CSF	A critical hematopoietic growth factor and immune modulator. Although GM-CSF is produced locally, it can act in a paracrine fashion to recruit circulating neutrophils, monocytes, and lymphocytes to enhance their functions in host defense (Shi et al. 2006). GM-CSF is a product of cells activated during inflammatory or pathologic conditions and mediates differentiation to other states that participate in immune responses (Ushach and Zlotnik 2016).
IFN-γ	A cytokine that is critical for innate and adaptive immunity; involved in tumor control (Schoenborn and Wilson 2007).
IL-1α	A potent inflammatory cytokine that activates the inflammatory process, and its signaling causes devastating diseases manifested by severe acute or chronic inflammation. IL-1α is expressed in many cell types, in healthy tissues at steady state, and its expression can be increased in response to growth factors and pro-inflammatory or stress-associated stimuli (Di Paolo and Shayakhmetov 2016).
IL-6	A pro-inflammatory cytokine that is involved in haematopoiesis, and is critical in the final maturation of B-cells into antibody-producing plasma cells (Kishimoto 2010). IL-6 is also produced by osteoblasts and found to induce bone resorption both alone and together with other bone-resorbing agents (Ishimi et al. 1990).
MMP-3	Involved in the breakdown of the extracellular matrix. MMP-3 has been linked to the cleaving of aggrecan, collagen type II, IX, and X as well as activating other metalloproteinases such as pro-MMP-1, pro-MMP-8, pro-MMP-9 and pro-MMP-13 (Sun et al. 2014).

MMP-7	Involved with the proteolytic cleavage of extracellular matrix and basement membrane proteins, such as fibronectin, collagen type IV, laminin, elastin, entactin, osteopontin, and cartilage proteoglycan aggregates. MMP-7 also activates other MMPs, such as proMMP-2 and proMMP-9, to facilitate tumor invasion and seems to mediate the proteolytic processing of tumor necrosis factor precursor and urokinase plasminogen activator (Yokoyama et al. 2008).
PAI-1	An important component of the plasminogen/plasmin system. PAI-1 down regulates fibrinolysis by limiting the production of plasmin. Also, it has been found that increased PAI-1 levels reduce the efficacy of thrombolytic therapy by preventing or retarding clot dissolution (Gils and Declerck 2004).
TGF-β1	A product of neoplastic and hemopoietic cells. It is a bifunctional regulator of the immune response. TGF-beta stimulates monocyte migration and its levels may induce synthesis of monocyte growth factors, including IL-1, which can promote tissue repair by regulating fibrosis and angiogenesis (Wahl et al. 1988).
TIMP-1	A glycoprotein that is a key regulator of the metalloproteinases that degrade the extracellular matrix and shed cell surface molecules. TIMP-1 has biological activities that are independent of metalloproteinases including: effects on cell growth and differentiation, cell migration, anti-angiogenesis, anti- and pro-apoptosis, and synaptic plasticity (Brew and Nagase 2010).
TNF-α	A potent inflammatory mediator that is central to the inflammatory action of the innate immune system, including induction of cytokine production, activation or expression of adhesion molecules, and growth stimulation (Turner et al. 2014).
VE-cadherin	An adhesive transmembrane protein specifically expressed at interendothelial junctions. VE-cadherin is dispensable for endothelial homophilic adhesion but is required for vascular morphogenesis (Gory-Faure et al. 1999).
VEGF	It is a mediator of angiogenesis and inflammation which are closely integrated processes in a number of physiological and pathological conditions including obesity, psoriasis, autoimmune diseases and tumor (Shaik-Dasthagirisaheb et al. 2013).

Appendix Table 2: Pre-processing statistics prior to running MFSDA. The clinical **(A)** and biological **(B)** variables' Pearson correlations to the principal component scores are shown along with their respective p-values. Percentages of the variance of the biomarkers explained by the principal component scores are listed to demonstrate the variance of the biomarkers explained by the principal component scores. TMJOA and control clinical and biological variances are all explained in the first two principal component scores except TMJOA saliva biomarkers, where the first principal component score explains 99.6% of the variance. MFSDA, multivariate functional shape data analysis; TMJOA, temporomandibular joint osteoarthritis; PC, principal component.

A		**Principal Component Scores and Percentages**					
Clinical Variables	**Status**	**Pearson Correlation to the 1st PC Score**	**p-value**	**Percentage**	**Pearson Correlation to the 2nd PC Score**	**p-value**	**Percentage**
Begin Pain Years	TMJOA	0.472	0.056	65.007	-0.232	0.369	28.897
Current Facial Pain Rate	TMJOA	0.376	0.137	65.007	-0.114	0.664	28.897
Facial Worst Pain Rate	TMJOA	0.169	0.517	65.007	0.105	0.688	28.897
Average Rate Six Months	TMJOA	0.224	0.387	65.007	0.194	0.455	28.897
Pain Location	TMJOA	0.050	0.849	65.007	-0.306	0.232	28.897
Range Without Pain Mouth Opening†	TMJOA	-0.058	0.824	65.007	0.998	0.000***	28.897
Range Unassisted Mouth Opening†	TMJOA	0.996	0.000***	65.007	-0.029	0.911	28.897
Range Assisted Mouth Opening†	TMJOA	0.994	0.000***	65.007	0.076	0.772	28.897
Headaches	TMJOA	0.395	0.116	65.007	0.222	0.392	28.897
Muscle Soreness	TMJOA	0.801	0.000***	65.007	0.052	0.844	28.897

B			**Principal Component Scores and Percentages**					
Biological Variables	**Fluid**	**Status**	**Pearson Correlation to the 1st PC Score**	**p-value**	**Percentage**	**Pearson Correlation to the 2nd PC Score**	**p-value**	**Percentage**
ANG	Serum	TMJOA	-0.366	0.149	84.452	0.378	0.135	14.661
MMP3	Serum	TMJOA	-0.034	0.897	84.452	0.999	0.000***	14.661
MMP7	Serum	TMJOA	0.411	0.101	84.452	0.618	0.008**	14.661
PAI-1	Serum	TMJOA	0.323	0.206	84.452	-0.172	0.509	14.661
TIMP-1	Serum	TMJOA	0.214	0.408	84.452	-0.089	0.734	14.661
VE-cadherin	Serum	TMJOA	0.999	0.000***	84.452	0.005	0.986	14.661
6Ckine	Serum	TMJOA	0.406	0.106	84.452	0.066	0.802	14.661
CXCL16	Serum	TMJOA	-0.143	0.584	84.452	0.713	0.001**	14.661
ENA-78	Serum	TMJOA	0.208	0.424	84.452	0.031	0.905	14.661
IL-1α	Serum	TMJOA	0.276	0.283	84.452	-0.074	0.777	14.661
VEGF	Serum	TMJOA	0.516	0.034*	84.452	0.074	0.778	14.661
ANG	Saliva	TMJOA	0.159	0.542	99.597			
MMP3	Saliva	TMJOA	0.988	0.000***	99.597			
MMP7	Saliva	TMJOA	0.602	0.011*	99.597			
PAI-1	Saliva	TMJOA	0.947	0.000***	99.597			
TIMP-1	Saliva	TMJOA	0.184	0.479	99.597			
VE-cadherin	Saliva	TMJOA	0.999	0.000***	99.597			
6Ckine	Saliva	TMJOA	0.979	0.000***	99.597			
CXCL16	Saliva	TMJOA	0.301	0.240	99.597			
ENA-78	Saliva	TMJOA	0.075	0.775	99.597			
IL-1α	Saliva	TMJOA	0.393	0.119	99.597			

VEGF	Saliva	TMJOA	0.133	0.610	99.597			
ANG	Serum	Control	0.383	0.129	78.423	0.526	0.030*	18.881
MMP3	Serum	Control	0.652	0.005**	78.423	0.758	0.000***	18.881
MMP7	Serum	Control	0.070	0.789	78.423	0.104	0.690	18.881
PAI-1	Serum	Control	0.198	0.447	78.423	-0.179	0.491	18.881
TIMP-1	Serum	Control	-0.118	0.651	78.423	0.101	0.700	18.881
VE-cadherin	Serum	Control	0.979	0.000***	78.423	-0.203	0.435	18.881
6Ckine	Serum	Control	0.132	0.613	78.423	-0.031	0.905	18.881
CXCL16	Serum	Control	0.575	0.016	78.423	0.629	0.007**	18.881
ENA-78	Serum	Control	-0.067	0.799	78.423	-0.216	0.404	18.881
IL-1α	Serum	Control	0.698	0.002**	78.423	0.426	0.088	18.881
VEGF	Serum	Control	0.514	0.035*	78.423	-0.175	0.501	18.881
ANG	Saliva	Control	0.467	0.059	66.535	0.495	0.044*	19.696
MMP3	Saliva	Control	-0.065	0.805	66.535	0.507	0.038*	19.696
MMP7	Saliva	Control	0.385	0.127	66.535	0.852	0.000***	19.696
PAI-1	Saliva	Control	-0.092	0.724	66.535	-0.473	0.055	19.696
TIMP-1	Saliva	Control	0.311	0.224	66.535	-0.421	0.093	19.696
VE-cadherin	Saliva	Control	0.989	0.000***	66.535	-0.021	0.936	19.696
6Ckine	Saliva	Control	0.751	0.001**	66.535	-0.067	0.798	19.696
CXCL16	Saliva	Control	0.247	0.340	66.535	0.589	0.013*	19.696
ENA-78	Saliva	Control	0.658	0.004**	66.535	0.556	0.021	19.696
IL-1α	Saliva	Control	-0.114	0.663	66.535	0.534	0.027*	19.696
VEGF	Saliva	Control	0.214	0.410	66.535	-0.184	0.479	19.696

* p-value <.05; ** p-value <.01 *** p-value <.001

Appendix Table 3: Pre-processing statistics prior to running MFSDA. Clinical **(A)** and biological **(B)** variables' descriptive statistics are shown. MFSDA, multivariate functional shape data analysis; TMJOA, temporomandibular joint osteoarthritis; SD, standard deviation.

A	**Descriptive Statistics**		
Clinical Variables	**Status**	**Median**	**Mean +/- SD**
Begin Pain Years	TMJOA	4	4.31+/-3.28
Current Facial Pain Rate	TMJOA	2	2.41+/-2
Facial Worst Pain Rate	TMJOA	7	6.59+/-2.58
Average Rate Six Months	TMJOA	6	5.18+/-2.81
Pain Location	TMJOA	3	2.59+/-0.80
Range Without Pain Mouth Opening†	TMJOA	43	39.52+/-12.40
Range Unassisted Mouth Opening†	TMJOA	39	37+/-12.38
Range Assisted Mouth Opening†	TMJOA	39	35.71+/-11.64
Headaches	TMJOA	2	1.59+/-1.06
Muscle Soreness	TMJOA	1	1.12+/-1.11

B		**Descriptive Statistics**			
Biological Variables		**TMJOA**		**Control**	
	Fluid	**Median**	**Mean +/- SD**	**Median**	**Mean +/- SD**
ANG	Serum	641.3	687.35+/-143.19	725.1	744.18+/-256.37
MMP3	Serum	13802.4	18268.53+/-11637.05	11425	15544.65+/-14575.85
MMP7	Serum	1592.1	2370.67+/-2084.7	1954.5	2073.57+/-905.53
PAI-1	Serum	1669.4	1859.25+/-935.76	1800.4	1796.83+/-688.27
TIMP-1	Serum	5234.1	5611.89+/-1381.67	6318.1	6131.86+/-2080.85
VE-cadherin	Serum	30751.1	41532.04+/-29314.92	35490.3	40547.84+/-22440.97
6Ckine	Serum	2031	2250.56+/-1729.19	2515.9	3566.02+/-3768.47
CXCL16	Serum	2241.2	2588.89+/-849.98	2948.3	3188.02+/-1467.02
ENA-78	Serum	771.7	1116.04+/-925.09	1192.7	1196.32+/-755.53
IL-1α	Serum	40	53.43+/-62.81	6.4	75.17+/-128.75
VEGF	Serum	576.9	848.95+/-777.27	763.7	880.74+/-483.75
ANG	Saliva	650	652.62+/-181.33	686.1	676.61+/-159.83
MMP3	Saliva	243.5	983.51+/-2293.37	176.8	1230.55+/-3232.02
MMP7	Saliva	11083.5	12208.77+/-6946.86	11773.5	12443.19+/-5792.83
PAI-1	Saliva	3.4	21.31+/-65.22	2.8	32.11+/-55.27
TIMP-1	Saliva	4387.2	3789.03+/-1683.22	4003.4	3596.59+/-1806.88
VE-cadherin	Saliva	4252.7	34968.17+/-103234.57	2559	6974.58+/-11014.47
6Ckine	Saliva	98.4	2570.11+/-9443.61	103	429.53+/-815.66
CXCL16	Saliva	186	489.58+/-614.68	343.9	352.71+/-220.88
ENA-78	Saliva	7185.1	7657.81+/-2539.35	5652.4	6569.43+/-6168.53
IL-1α	Saliva	331.8	743.88+/-998.83	315.1	922.59+/-1348.26
VEGF	Saliva	398.8	445.19+/-272.97	294.9	350.62+/-225.09

† : Measured in millimeters (mm)

Appendix Figure 1

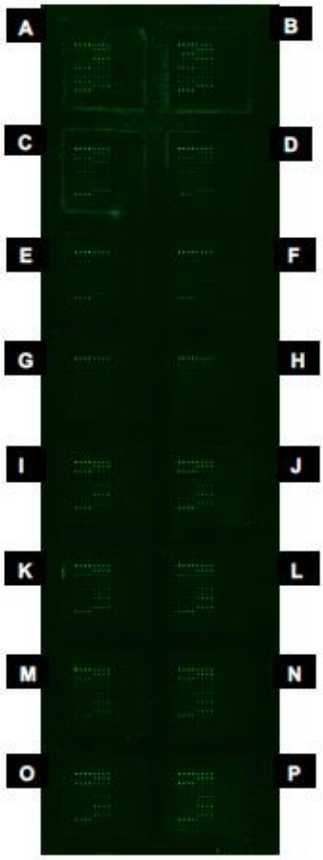

Appendix Figure 1: The RayBiotech Quantibody® glass slides used that had 16 wells each with identical cytokine antibody arrays. They were run under fluorescence laser scanner equipped with a Cy3 wavelength (green channel), which allowed for quantification of the concentration of the protein of interest in the solution (RayBiotech 2018). This figure's specific glass slide: wells **A-G** are the standards; well **H** is the negative control; wells **K** and **L**; **M** and **N**; and **O** and **P** are the first three de-identified patients where duplicates were run in each row.

Appendix Figure 2

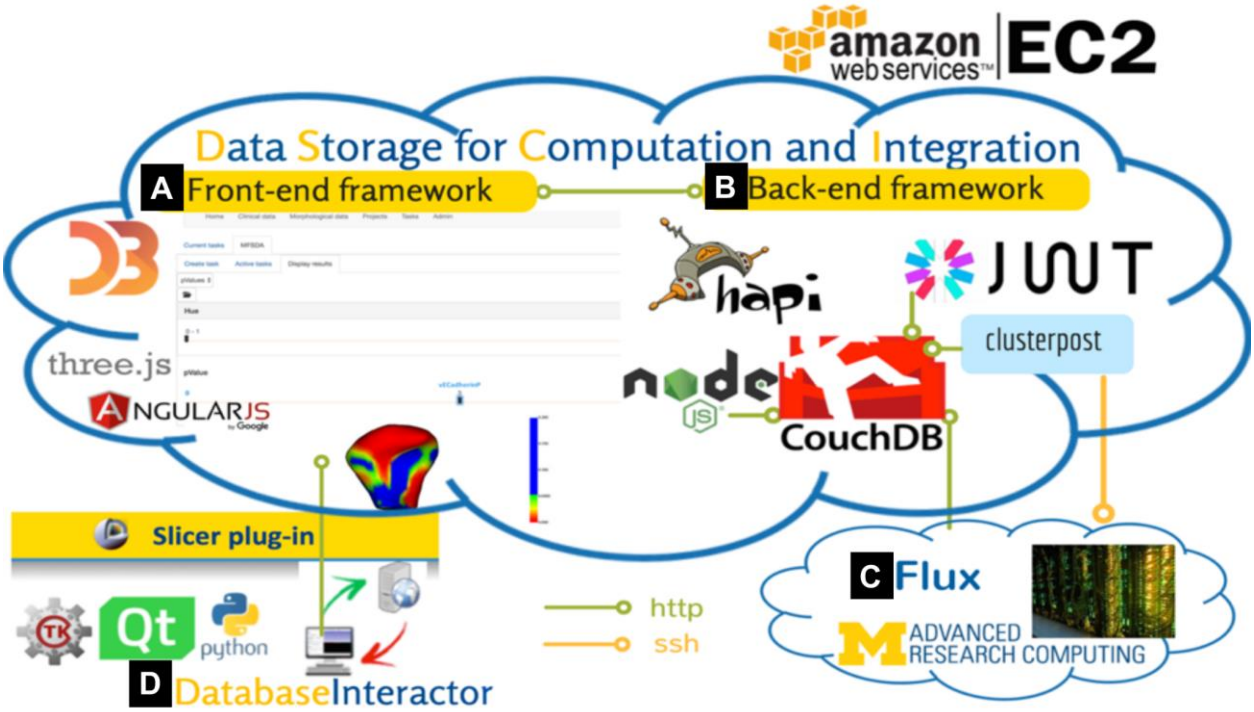

Appendix Figure 2: (A) The front end of the application is based on Angular.js, the visualization is done using D3.js and 3D visualization of morphological data was accomplished with Threejs using a WebGL renderer. **(B)** The web-based system has been designed with Node and Hapi for the back-end framework, Couchdb for the storage and JWT for the authentication system. A plug-in has been developed for Node, allowing storage and retrieval of user information, as well as JWT encryption exchanged with the user upon login. Clusterpost was integrated to submit tasks to remote computing grids using the stored data. The application was hosted using Amazon web services or the Elastic Compute Cloud. (C) The computation was done using 4 cores with 16 GB of total RAM to run the MFSDA Matlab package stored on Flux. Flux consists of approximately 27,000 cores. (D) DatabaseInteractor is a 3D Slicer plug-in used to manage patient data. 3D, three-dimensional; EC2, Amazon Elastic Compute Cloud; JWT, JSON Web Token; GB, gigabyte; RAM, random access memory; MFSDA, multivariate functional shape data analysis.

Appendix Figure 3

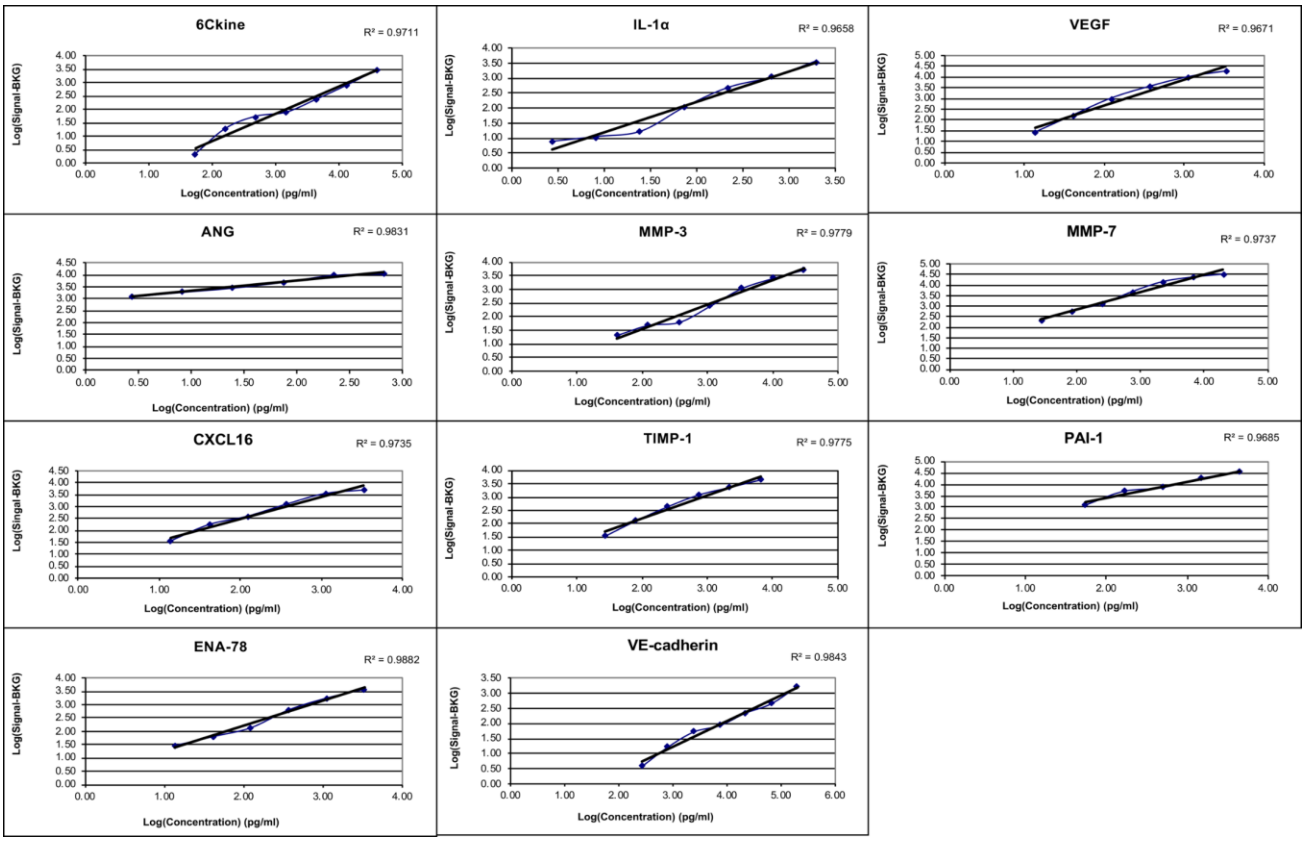

Appendix Figure 3: Shown above every graph are the standard concentrations and the signal minus background (Signal-BKG) concentrations for the 11 biomarkers. Positive controls for each biomarker were included in each array, and the array data obtained from densitometry were entered into the appropriate cells of the corresponding analysis tool, which plotted the standard curve for each analysis in addition to performing background subtraction/normalization. The logs of the standard concentrations and the logs of the Signal-BKG concentrations are taken and graphed. A log-log regression graph is plotted, and the coefficient of determination is calculated. BKG, background.

Appendix References:

Abel S, Hundhausen C, Mentlein R, Schulte A, Berkhout TA, Broadway N, Hartmann D, Sedlacek R, Dietrich S, Muetze B. 2004. The transmembrane cxc-chemokine ligand 16 is induced by ifn-γ and tnf-α and shed by the activity of the disintegrin-like metalloproteinase adam10. The Journal of Immunology. 172(10):6362-6372.

Benjamini Y. 2010. Discovering the false discovery rate. Journal of the Royal Statistical Society: series B (statistical methodology). 72(4):405-416.

Quantibody multiplex elisa array. 2018. [accessed]. https://www.raybiotech.com/quantibody-multiplex-elisa-array/.

Brew K, Nagase H. 2010. The tissue inhibitors of metalloproteinases (timps): An ancient family with structural and functional diversity. Biochimica et biophysica acta. 1803(1):55-71.

Campbell JJ, Bowman EP, Murphy K, Youngman KR, Siani MA, Thompson DA, Wu L, Zlotnik A, Butcher EC. 1998. 6-c-kine (slc), a lymphocyte adhesion-triggering chemokine expressed by high endothelium, is an agonist for the mip-3β receptor ccr7. The Journal of Cell Biology. 141(4):1053-1059.

Chang MS, McNinch J, Basu R, Simonet S. 1994. Cloning and characterization of the human neutrophil-activating peptide (ena-78) gene. J Biol Chem. 269(41):25277-25282.

de Dumast P. Shapevariationanalyzer (sva) source code extension. 2017. github.com; [accessed]. https://github.com/Slicer/ExtensionsIndex/blob/master/ShapeVariationAnalyzer.s4ext.

de Dumast P, Mirabel C, Paniagua B, Yatabe M, Ruellas A, Tubau N, Styner M, Cevidanes L, Prieto JC. 2018. Sva: Shape variation analyzer. Proceedings of SPIE--the International Society for Optical Engineering. 10578:105782H.

Di Paolo NC, Shayakhmetov DM. 2016. Interleukin 1α and the inflammatory process. Nature Immunology. 17(8):906.

Gao X, Xu Z. 2008. Mechanisms of action of angiogenin. Acta Biochimica et Biophysica Sinica. 40(7):619-624.

Gils A, Declerck PJ. 2004. Plasminogen activator inhibitor-1. Current Medicinal Chemistry. 11(17):2323-2334.

Gory-Faure S, Prandini MH, Pointu H, Roullot V, Pignot-Paintrand I, Vernet M, Huber P. 1999. Role of vascular endothelial-cadherin in vascular morphogenesis. Development. 126(10):2093-2102.

Grimsholm O, Rantapää-Dahlqvist S, Dalén T, Forsgren S. 2008. Bdnf in ra: Downregulated in plasma following anti-tnf treatment but no correlation with inflammatory parameters. Clinical Rheumatology. 27(10):1289-1297.

Gunn MD, Tangemann K, Tam C, Cyster JG, Rosen SD, Williams LT. 1998. A chemokine expressed in lymphoid high endothelial venules promotes the adhesion and chemotaxis of naive t lymphocytes. Proc Natl Acad Sci U S A. 95(1):258-263.

Ishimi Y, Miyaura C, Jin CH, Akatsu T, Abe E, Nakamura Y, Yamaguchi A, Yoshiki S, Matsuda T, Hirano T. 1990. Il-6 is produced by osteoblasts and induces bone resorption. The Journal of Immunology. 145(10):3297-3303.

Kaczor-Urbanowicz KE, Trivedi HM, Lima PO, Camargo PM, Giannobile WV, Grogan TR, Gleber-Netto FO, Whiteman Y, Li F, Lee HJ. 2018. Salivary exrna biomarkers to detect gingivitis and monitor disease regression. Journal of Clinical Periodontology. 45(7):806-817.

Keelan J, Yang J, Romero R, Chaiworapongsa T, Marvin K, Sato T, Mitchell M. 2004. Epithelial cell-derived neutrophil-activating peptide-78 is present in fetal membranes and amniotic fluid at increased concentrations with intra-amniotic infection and preterm delivery. Biology of Reproduction. 70(1):253-259.

Kishimoto T. 2010. Il-6: From its discovery to clinical applications. International Immunology. 22(5):347-352.

Kras JV, Weisshaar CL, Quindlen J, Winkelstein BA. 2013. Brain-derived neurotrophic factor is upregulated in the cervical dorsal root ganglia and spinal cord and contributes to the maintenance of pain from facet joint injury in the rat. Journal of Neuroscience Research. 91(10):1312-1321.

Liote F, Champy R, Moenner M, BOVAL-BOIZARD B, Badet J. 2003. Elevated angiogenin levels in synovial fluid from patients with inflammatory arthritis and secretion of angiogenin by cultured synovial fibroblasts. Clinical & Experimental Immunology. 132(1):163-168.

Ludlow J, Timothy R, Walker C, Hunter R, Benavides E, Samuelson D, Scheske M. 2014. Effective dose of dental cbct—a meta analysis of published data and additional data for nine cbct units. Dentomaxillofacial Radiology. 44(1):20140197.

Schoenborn JR, Wilson CB. 2007. Regulation of interferon-γ during innate and adaptive immune responses. Advances in Immunology. Academic Press. p. 41-101.

Shaik-Dasthagirisaheb YB, Varvara G, Murmura G, Saggini A, Potalivo G, Caraffa A, Antinolfi P, Tete S, Tripodi D, Conti F et al. 2013. Vascular endothelial growth factor (vegf), mast cells and inflammation. International Journal of Immunopathology and Pharmacology. 26(2):327-335.

Shi Y, Liu CH, Roberts AI, Das J, Xu G, Ren G, Zhang Y, Zhang L, Yuan ZR, Tan HS et al. 2006. Granulocyte-macrophage colony-stimulating factor (gm-csf) and t-cell responses: What we do and don't know. Cell Research. 16(2):126-133.

Soto H, Wang W, Strieter RM, Copeland NG, Gilbert DJ, Jenkins NA, Hedrick J, Zlotnik A. 1998. The cc chemokine 6ckine binds the cxc chemokine receptor cxcr3. Proceedings of the National Academy of Sciences. 95(14):8205-8210.

Stehman SV. 1997. Selecting and interpreting measures of thematic classification accuracy. Remote Sensing of Environment. 62(1):77-89.

Sun S, Bay-Jensen A-C, Karsdal MA, Siebuhr AS, Zheng Q, Maksymowych WP, Christiansen TG, Henriksen K. 2014. The active form of mmp-3 is a marker of synovial inflammation and cartilage turnover in inflammatory joint diseases. BMC Musculoskeletal Disorders. 15(1):93.

Turner MD, Nedjai B, Hurst T, Pennington DJ. 2014. Cytokines and chemokines: At the crossroads of cell signalling and inflammatory disease. Biochimica et Biophysica Acta (BBA) - Molecular Cell Research. 1843(11):2563-2582.

Ushach I, Zlotnik A. 2016. Biological role of granulocyte macrophage colony-stimulating factor (gm-csf) and macrophage colony-stimulating factor (m-csf) on cells of the myeloid lineage. Journal of Leukocyte Biology. 100(3):481-489.

Wahl SM, Hunt DA, Wong HL, Dougherty S, McCartney-Francis N, Wahl LM, Ellingsworth L, Schmidt JA, Hall G, Roberts AB. 1988. Transforming growth factor-beta is a potent immunosuppressive agent that inhibits il-1-dependent lymphocyte proliferation. The Journal of Immunology. 140(9):3026-3032.

Yokoyama Y, Grünebach F, Schmidt SM, Heine A, Häntschel M, Stevanovic S, Rammensee H-G, Brossart P. 2008. Matrilysin (mmp-7) is a novel broadly expressed tumor antigen recognized by antigen-specific t cells. Clinical Cancer Research. 14(17):5503-5511.